Enhanced Microwave Absorption Properties of Y Doped $BiFeO_3$

Bambang Soegijono[1*], Suharno[2], Rahmatul Hidayati[1] , Dwita Suastiyanti.[3]

[1]Department of Physics, University of Indonesia, Depok, Indonesia 16424

[2]Department of Physics Education, University of Ahmad Dahlan, Yogyakarta, Indonesia 55161,

[3]Mechanical Department of Indonesia Institute of Technology – Serpong, Indonesia.

**Corresponding author's email : bambangsg11 [AT] yahoo.com*

ABSTRACT— Polycrystalline $Bi_{1-x}Y_xFeO_3$ with x = 0, 0.06, and 0.12 wt% have been synthesized by sol–gel autocombustion method. The gel have been heated at 150°C for 3 h, dried, grounded and followed by calcination at 750°C for 5 h. The X-ray diffraction (XRD) patterns of samples are indexed and well matched with rhombohedral structure (R3c). The samples of $Bi_{1-x}Y_xFeO_3$, (x = 0, 0.06, 0.12) show impuruties of $Bi_{25}Fe_2O_{39}$ in small amount. The decrease intensity in the splitting of (104) and (110) peaks around 2θ = 32° indicates the reduction of the rhombohedral phase transform to orthorhombic phase. The scanning electron microscopy (SEM) shows doping Yttrium reduce particle size. The M-H curve measured with SQUID results saturation magnetization at 60 K of pure (3.36 emu/g) and Y doped (19.54 emu/g), the saturation magnetization at 300 K of pure (3.11 emu/g) and Y doped (14.73 emu/g). Reflection Loss (RL) of of $Bi_{1-x}Y_xFeO_3$/Silicon Rubber composite increase with optimum value of -37.23 dB at 10.85 GHz.

Keywords— Multiferroic, BiFeO3, Microwave absorption, Doped

1. INTRODUCTION

Electromagnetic interference (EMI) has become serious problems due to many communication devices which utilize gigahertz range microwave radiation. One of many technique to prevent EMI is the use of microwave absorption materials. [1] . In applications, microwave absorption materials should possess wide waveband and strong absorption, light weight, thin thickness, suitable physical–mechanical properties, simple operation and cheap. [2,3]. According to dissipation mechanisms, microwave absorption materials can be devided into two types: dielectric loss and magnetic loss. The fundamental principles [4,5] for microwave absorption in materials are deduced based on electromagnetic theory for single layer, monocomponent absorption materials. The keys lie in firstly, transmitting the microwave into the material rather than being reflected on the surface, which is referred as surface impedance match; then, consuming the entered microwave to the greatest extent which is referred as the attenuation property.

Multiferroic materials,such as $BiFeO_3$ (BFO) which combine ferromagnetic and ferroelectric features, have attracted much attention because of their potential applications in data storage, spin valves, quantum electromagnets, and microelectronic devices [6–10]. Besides these applications, BFO might be a promising candidate of absorbing materials due to the coexistence of the ferroelectric and ferromagnetic order. For microwave absorption, the attenuation is dominated by electric and magnetic dipoles, so excellent absorbing materials should possess a good electromagnetic match between the dielectric loss and magnetic loss. Perovskite-type $BiFeO_3$ (BFO) is the most important room temperature multiferroic material due to its high ferroelectric Curie temperature (T_C=1103K) [11] and G-type anti-ferromagnetic Ne´el temperature (T_N = 647 K), [12] which are beneficial for many applications..

However, the microwave absorption properties are the weak magnetization caused by the space modulated spin structure in the BFO crystal. For the purpose of improving the electromagnetic match of BFO nanomaterials, in this research , we perform the investigationon the crystal structure ,magnetic, dielectric, and microwave absorption properties in the X-Band of Ytrium doped BFO. The enhancement of ferromagnetism of Yitrium doped BFO and microwave absorption properties are apparently expected.

2. MATERIALS AND METHOD

Polycrystalline $Bi_{1-x}Y_xFeO_3$ with x = 0, 0.06, and 0.12 wt% have been synthesized by sol–gel autocombustion method. The analytical grade of $Bi(NO_3)_2.5H_2O$, $Fe(NO_3)_3.9H_2O$, and $Y(NO_3)_3$ $.6H_2O$ in appropriate amounts, have been used to prepare precursor solutions by dissolving them in Citric Acid $C_7H_8O_7$ solution as fuel. The result solution was transparent, brownish, and clear. The mixture was stirred for 3 – 4 hours at 80°C on a hot plate to accelerate the gel formation. Furthermore, the gel have been heated at 150 °C for 3 h. The samples were grounded and followed by calcination at 750°C for 5 hours.

The structure of $Bi_{1-x}Y_xFeO_3$ were investigated using X-ray diffraction technique at room temperature (XRD Phillips model with Cu-Kα radiation, wave length λ=1.5406 Å). The morphology of the samples were examined by Field Emmision Scanning electron microscopy (FE-SEM) FEI F50 couple with EDS. The magnetic properties of the samples were measured with Superconducting Quantum Interference Device (SQUID) with the external magnetic field between – 3 kOe to + 3 kOe at 60 K and 300 K. The composite samples for electromagnetic properties measurement were prepared by mixing $Bi_{1-x}Y_xFeO_3$ (x = 0, 0.06, 0.12 wt%) and the 50 wt% Silicon rubber. Then the mixture was pressed into rectangle square shape with size 25 x 12.5 x 1.5 mm to fit the sample holder. The Reflection loss were measured using Vector Network Analyzer R3770 type at frequency range 8.2 – 12.4 GHz (X band). The complex permittivity and permeability of the compound samples were calculated from parameter complex reflection coefficient S_{11} and complex transmission coefficient S_{21}.

3. RESULTS AND DISCUSSION

3.1 Structure of $Bi_{1-x}Y_xFeO_3$ (x = 0, 0.06, 0.12 wt%)

Figure 1 shows the XRD pattern of the as-prepared $Bi_{1-x}Y_xFeO_3$ (x = 0, 0.06, 0.12wt%) . The XRD reflection peaks of the samples are indexed and well matched with rhombohedral structure (R3c) and impurities indicated by * such as $Bi_{25}Fe_2O_{39}$ in small amount.

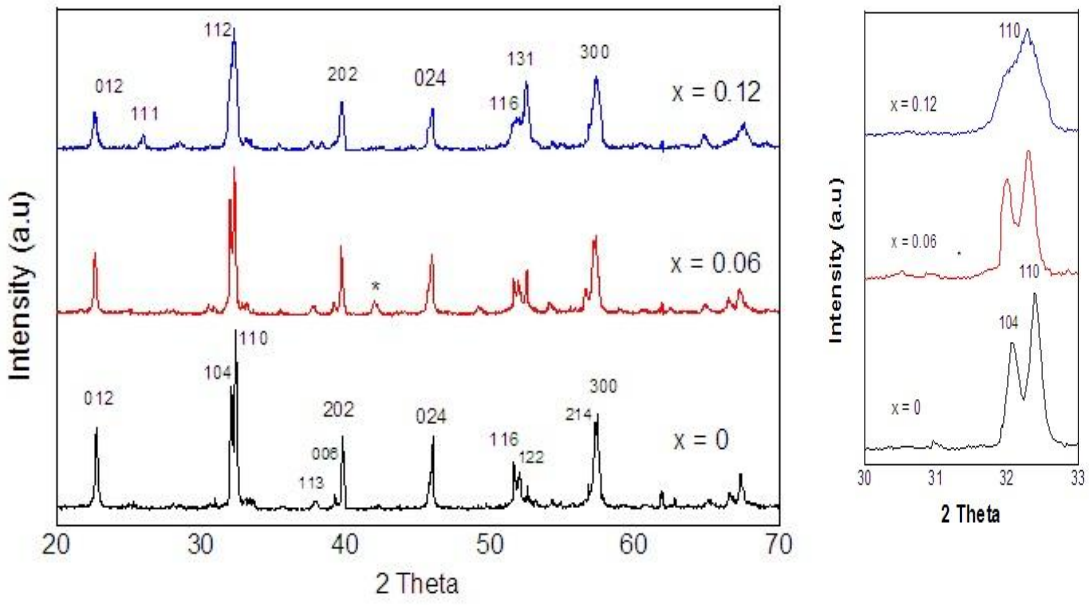

Figure 1 : The X-ray diffraction (XRD) patterns of $Bi_{1-x}Y_xFeO_3$ (x = 0, 0.06, 0.12 wt%)

The decrease intensity of (104) peak clearly show the structural transformation from rhombohedral to orthorhombic due to increase in Y content in $BiFeO_3$. The structural transformation from rhombohedral to orthorhombic takes place as Ytrium doping increase from x = 0.06 to 0.12wt%.

The results of Rietveld refinement of the $Bi_{1-x}Y_xFeO_3$ (x = 0, 0.06, 0.12wt%) show at **Table 1** and the crystallite size were determined from FWHM for all samples using Scherrer's equation.

Table 1: The Rhombohedral R3c structure of $Bi_{1-x}Y_xFeO_3$ (x = 0, 0.06, 0.12 wt%)

Paramaters		x = 0	x = 0.06	x = 0.12
α, β, γ		90°, 90°, 120°	90°, 90°, 120°	90°, 90°, 120°
$a = b$ (Å)		5.5783	5.5877	5.5837
c(Å)		13.8552	13.8706	13.8371
Cell volume (Å^3)		373.3727	375.0565	373.6139
Atomic positions				
	Bi	0, 0, 1.0727	0, 0, -0.0198	0, 0, 1.4837
	Fe	0, 0, 1.3438	0, 0, 0.2110	0, 0, 1.7634
	O	2.3730, 1.2480, 2.4894	0.4838, -0.0722, 1.0048	-3.7815, 1.4100, 2.4338
Crystallite Size (nm)		63.75	54.23	48.96
Density (g/cm^3)		8.33	8.31	8.34

3.2 The Morphology of $Bi_{1-x}Y_xFeO_3$ (x = 0, 0.06, 0.12 wt%)

Figure 2. shows the scanning electron micrographs of sintered powders $Bi_{1-x}Y_xFeO_3$ (x = 0, 0.06, 0.12 wt%). The grains of the samples are not homogen in shape and their size and also exibit aglomeration. The morphology of Y 12 wt% doped BFO show smaller than others.

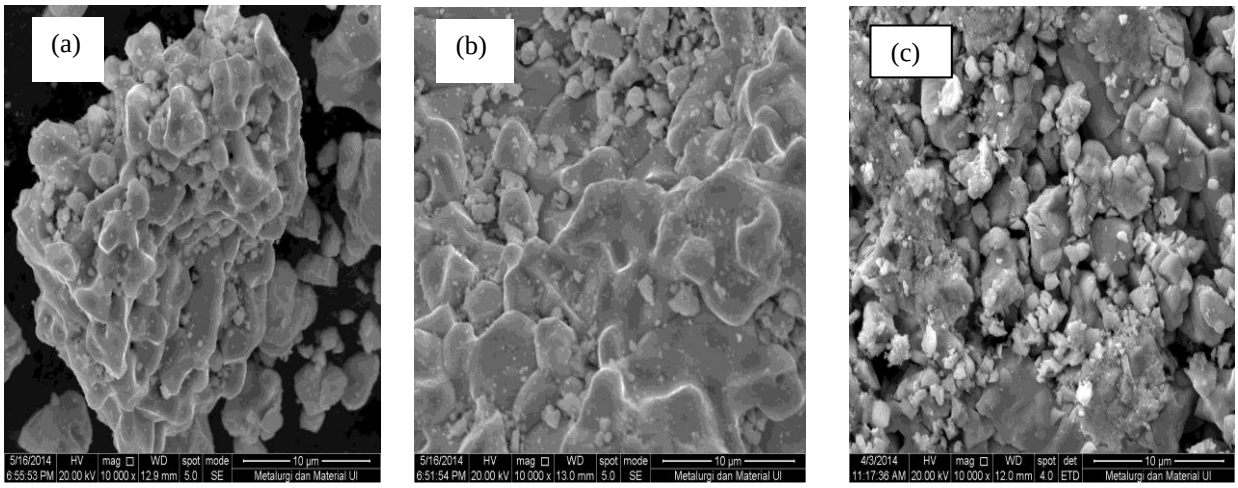

Figure 2 :. The Morphology of $Bi_{1-x}Y_xFeO_3$ (a) x = 0 (b) x = 0.06 (c) x = 0.12 wt%

It is clear that the grain growth found to be suppressed with increasing in Y content and better in densification process. The smaller grain size is probablely due to smaller size of Y^{3+} ions as compared to those of Bi^{3+} ions, and results in lattice contraction. The EDS of BiFeO3 confirms the presence of Bi, Fe, and O elements. The EDS analysis was carried out and the Bi : Fe mol ratio was found close to be 1:1 . The result show Bi 67.32%, Fe 17.49%, and O 14.04% wt%.

3.3 Magnetic Properties of $Bi_{1-x}Y_xFeO_3$ (x = 0, 0.06, 0.12 wt%)

The Magnetization versus Magnetic field M-H curve of $Bi_{1-x}Y_xFeO_3$ samples with x = 0, 0.06, 0.12 wt% are measured by means of SQUID with a magnetic field of 3 kOe at 60 K and 300 K as shown in **Figure 3**. The G-type Antiferromagnetic in BFO limits the higher magnetization. Saturation magnetization decrease as the temperature increase from 60 to 300 K and so does with increasing Yttrium doped $BiFeO_3$. The SQUID measured for pure and Y doped BFO at 60 K increases gradually with x reaching maximum value for x = 0.12 (3.36 emu/gr and 19.54 emu/g respectively). The coercivity (Hc) decreases with increasing temperature (60 to 300 K). The Coercivity (Hc) value of $BiFeO_3$ are small so that BFO is soft magnetic material.

The potential magnetization locked in the spin cycloid of the BFO can be released by destroying the cyclic spin structure upon Y doping. Remarkable enhancement in the coercivity (H_C) is observed with Y, which is a clear indication of the transition from antiferromagnetic to ferromagnetic behaviour. The M-H measured at 3 kOe increases linearly with *x* on the SQUID measurement.

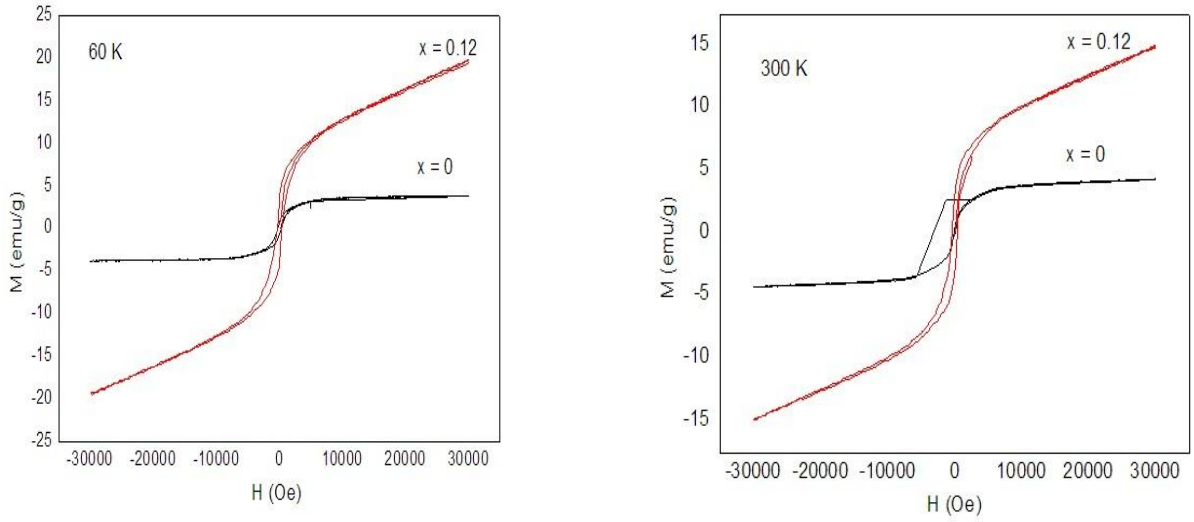

Figure 3 :. The loops hysterisis magnetic of pure and Y doped $BiFeO_3$ at 60 K and 300 K

Table 2. Show the Magnetic properties of Y doped BFO

Table 2:. The Magnetic properties of $Bi_{1-x}Y_xFeO_3$ (*x* = 0, 0.12)

x	60 K		300 K	
	M (emu/g)	Hc (Oe)	M (emu/g)	Hc (Oe)
0	3.36	819.71	3.11	757.85
0.12	19.54	448.52	14.73	386.65

3.4 Microwave Absorption Properties of $Bi_{1-x}Y_xFeO_3$ (x = 0, 0.06, 0.12wt%)

. The relative permeability ($\mu_r = \mu' + i\mu''$) and permitivity ($\varepsilon_r = \varepsilon' + i\varepsilon''$) value of the composites were determined from the parameters S_{11} and S_{21} measured in the frequency range of 8.2 – 12.4 GHz (X band). The Reflection Loss (RL) curves were calculated from the relative permeability and permitivity for a given frequency and absorber thickness by means of the following equations :

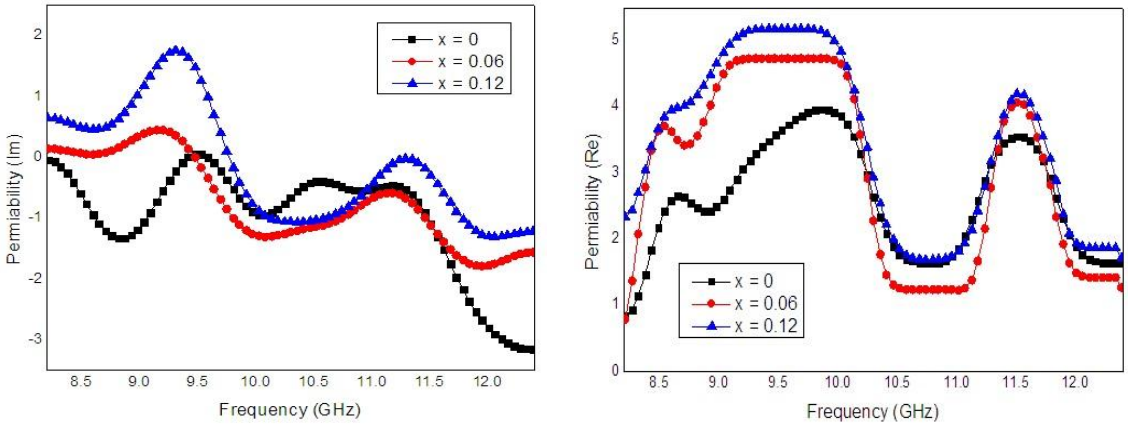

Figure 4 :. The Permeability (Im and Re) of $Bi_{1-x}Y_xFeO_3$/Silicone rubber composites,

x = 0, 0.06, 0.12wt%

$$Z_{RAM} = \sqrt{\frac{\mu_r}{\varepsilon_r}} tanh\left(j\frac{2\pi d}{c}\sqrt{\mu_r \varepsilon_r}\right) \quad (1)$$

$$RL\ (dB) = 20\ Log\left|\frac{Z_{RAM}-1}{Z_{RAM}+1}\right| \quad (2)$$

where *d* is the thickness of the absorber, *c* the velocity of light, Z_{RAM} is impedance of the absorber. **Figure 4** shows the real part (μ') and the imaginary part (μ'') of the relative permeability (μ_r) of the composites $BiFeO_3$/Silicone rubber, $Bi_{0.94}Y_{0.06}FeO_3$/silicone rubber and $Bi_{0.88}Y_{0.12}FeO_3$/silicone rubber in the 8.2 – 12.4 GHz range. It is interesting that the values of μ' are influenced by the Y doping. With increasing the Y content, the μ'' values are also increase.

Figure 5. shows the real part (ε') and the imaginary part (ε'') of the relative permitivity (ε_r) of the composites $BiFeO_3$/Silicone rubber, $Bi_{0.94}Y_{0.06}FeO_3$/silicone rubber, and $Bi_{0.88}Y_{0.12}FeO_3$/silicone rubber in the 8.2 – 12.4 GHz range. The relative permitivity (ε_r) of the composites $BiFeO_3$/Silicone rubber greather than $Bi_{0.88}Y_{0.12}FeO_3$/silicone rubber. The small value of ε'' indicated a higher resistivity of present composites compared with nanocrystal $Bi_{1-x}Y_xFeO_3$/Silicone rubber. In general, a high electrical resistivity is good for improving the microwave absoprtion properties

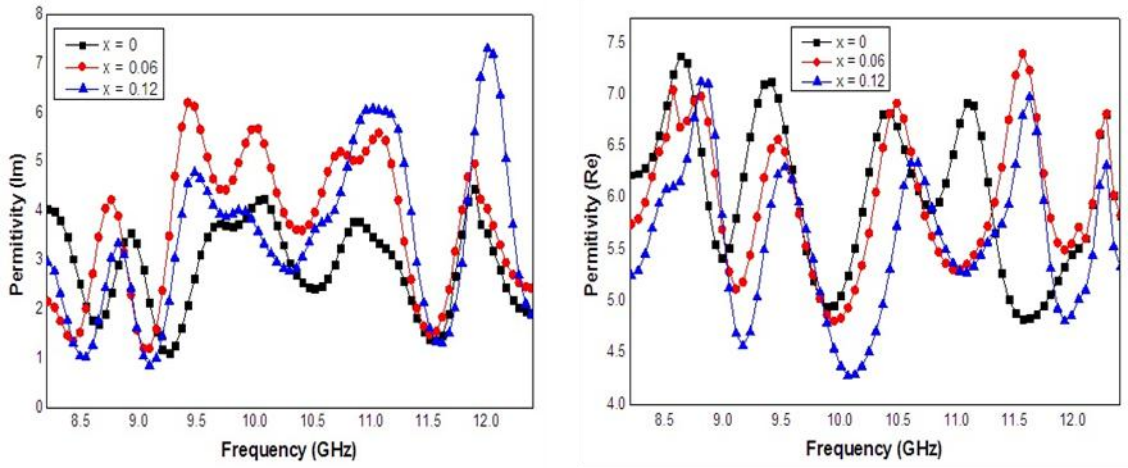

Figure 5. The Permitivity (Im and Re) of $Bi_{1-x}Y_xFeO_3$/Silicone rubber composites, x = 0, 0.06, 0.12 wt%

The generaly, the real part of complex permitivity represents the energy storage capacity. And the imaginary part of the complex permitivity and permeability account for the energy loss disipative mechanisms in the materials. The microwave absoprtion properties can be influenced by the magnetic loss and dielectric loss. The magnetic loss factor and the dielectric loss factor of $Bi_{1-x}Y_xFeO_3$/Silicone rubber composites are shown in **Figure 6**. A higher value of $\tan\delta$ indicates a higher loss.

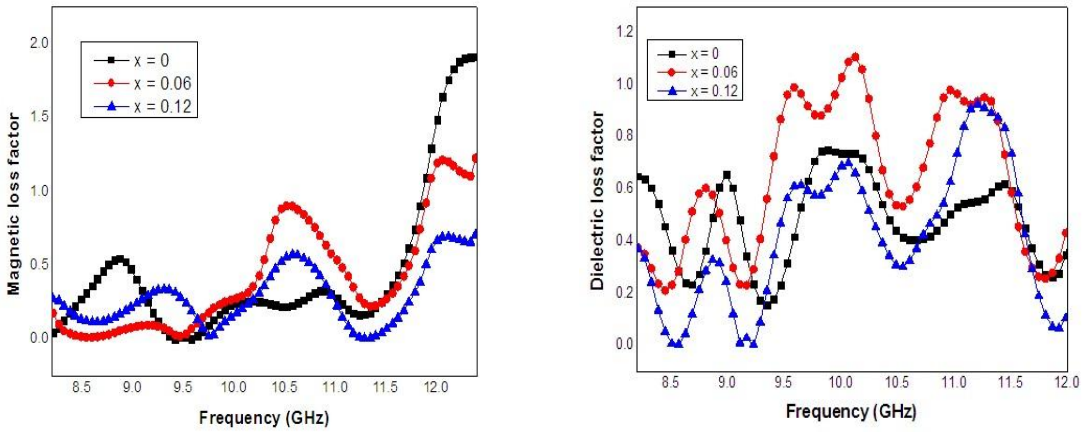

Figure 6 :. The Magnetic loss and Dielectric loss factor of $Bi_{1-x}Y_xFeO_3$/Silicone rubber composites, x = 0, 0.06, 0.12wt%

The magnetic loss factor ($\tan \delta_m$) and the dielectric loss factor ($\tan \delta_e$) were determined by :

$$\tan \delta_m = \frac{\mu''}{\mu'} \text{ and } \tan \delta_e = \frac{\varepsilon''}{\varepsilon'} \quad (3)$$

Figure 7 shows the Reflection Loss(RL) value of $Bi_{1-x}Y_xFeO_3$/Silicone rubber composites, x = 0, 0.06, 0.12 wt% as a function of frequency. For the sample $Bi_{0.88}Y_{0.12}FeO_3$/silicone rubber is optimum with RL value is -37.23 dB at 10.85 GHz so that RL of 12wt% Yttrium doped $BiFeO_3$ are excellent.

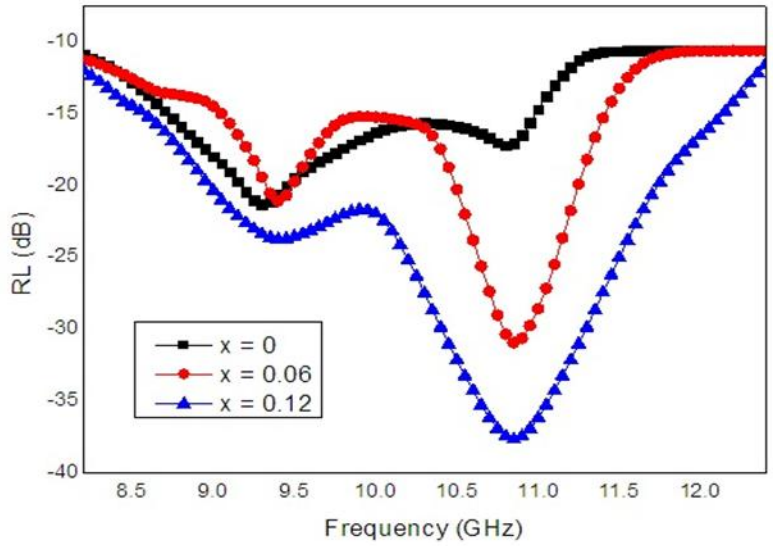

Figure 7 :. The Reflection loss (RL) of $Bi_{1-x}Y_xFeO_3$/Silicone rubber composites, x = 0, 0.06, 0.12 wt%

Microwave magnetic loss presents a clear increase due to the natural ferromagnetic resonance enhancement caused by Y substitution. The better microwave absorption properties are obtained owing to the fact that Ytrium substitution improves the electromagnetic match property.

4. CONCLUSION

Multiferroic $Bi_{1-x}Y_xFeO_3$ (x = 0, 0.06, 0.12wt%) nanoparticles with Y substitution have been successfully prepared with a sol gel auto combustion method. Ytrium doped Bismuth Ferrite powders have been rhombohedral structure changes to orthorhombic phase as the Ytrium doping increases on Bismuth site. The magnetization of the $Bi_{1-x}Y_xFeO_3$ samples increases with increasing doping level at room temperature. Microwave magnetic loss presents a clear increase due to the natural ferromagnetic resonance enhancement caused by Y substitution. The better microwave absorption properties are obtained owing to the fact that Ytrium substitution improves the electromagnetic match property and Y doped BFO is a promising materials as Microwave Absorption..

5. ACKNOWLEDGEMENT

The authors Thank Ministry of Research and Technology and Higher Education, The Republic of Indonesia for providing the SINas research grant 2015 (Grant No. 14/SEK/INSINAS/PPK/IV/2015)

6. REFERENCES

[1] Y. Naito, K. Suetake, Application of Ferrite to Electromagnetic Wave Absorber and its Characteristics , IEEE Trans. Microwave Theory Tech. 19 (1971) pp.65.

[2] I.M. De Rosa, A. Dinescu, F. Sarasini, M.S. Sarto, Effect of short carbon fibers and MWCNTs on microwave absorbing properties of polyester composites containing nickel-coated carbon fibers, Composites Science and Technology 70 (2010), pp.102–109.
[3] V.M. Petrov, V.V. Gagulin, Microwave absorbing materials, Inorganic Materials 37 (2001) pp.93–98.
[4] L.J. Deng, M.G. Han, Microwave absorbing performances of multiwalled carbon nanotube, Applied Physics Letters 91 (2007).
[5] J.B. Kim, S.K. Lee, C.G. Kim, Comparison study on the effect of carbon nano materials for single-layer microwave absorbers in X-band, Composites Science and Technology 68 (2008) pp.2909–2916.
[6] L.Wang,J.B.Xu,B.Gao,A.M.Chang,J.Chen,L.Bian,C.Y.Song, Synthesis of $BiFeO_3$ nanoparticles by a low-heating temperature solid state precursor method, Materials Research Bulletin 48(2013) pp.383–388.
[7] K.F.Wang, J.M.Liu, Z.F.Ren, Multiferroicity:the coupling between magnetic and polarization orders, Advances in Physics 58 (2009) pp.321–448.
[8] Y.Tokunaga,N.Furukawa,H.Sakai,Y.Taguchi,T.H.Arima, Y. Tokura,Composite domain walls in a multiferroic perovskite ferrite, NatureMaterials8(2009) pp.558–562.
[9] J.X.Zhang, Q.He,M.Trassin, W.Luo,D.Yi, M.D.Rossell, P.Yu, L. You, C.H.Wang, C.Y.Kuo, J.T.Heron, Z.Hu, R.J.Zeches, H.J. Lin, A.Tanaka, C.T.Chen, L.H.Tjeng, Y.H.Chu, R.Ramesh, Microscopic origin of the giant ferroelectric polarization in tetragonal-like BiFeO3, Physical Review Letters 107(2011) 147602.
[10] X.L.Yan, J.G.Chen, Y.F.Qi, J.R.Cheng, Z.Y.Meng, Hydrothermal synthesis and characterization of multiferroic $Bi_{1-x}La_x$ FeO_3 crystallites, Journal of theEuropean Ceramic Society 30(2010) pp. 265–269.
[11] D.C.Arnold, K.S.Knight, F.D.Morrison, P.Lightfoot, Ferroelectric–paraelectric transition in $BiFeO_3$: crystal structure of the orthorhombic b phase, Physical Review Letters 102 (2009) 27602.
[12] C.Michel, J.M.Moreau, G.D.Achenbach, R.Gerson, W.James, The atomic structure of $BiFeO_3$, Solid State Communications 7 (1969) pp.701–704.